NAD(P)H oxidase mimic for catalytic tumor therapy via deacetylase SIRT7-mediated AKT/GSK3β pathway

Qi Fang[a,b], Quanyi Liu[a,b], Zhimin Song[a,b], Xiaojun Zhang[b,*] and Yan Du[a,b,*]

[a.] State Key Laboratory of Electroanalytical Chemistry, Changchun Institute of Applied Chemistry, Chinese Academy of Sciences, Changchun, Jilin 130022, P. R. China.

[b.] School of Applied Chemistry and Engineering, University of Science & Technology of China, Hefei, Anhui 230026, P. R. China.

Experimental section

1. Chemicals and reagents

Imidazole, sucrose, sodium chloride (NaCl), cobaltous nitrate hexahydrate ($Co(NO_3)_2 \cdot 6H_2O$), and alcohol were purchased from Xilong Chemical Co., Ltd. (Shantou, China). NADH and NADPH were obtained from Bide Pharmatech Ltd (Shanghai, China). Superoxide dismutase was purchased from Shanghai Yuanye Bio-Technology Co., Ltd. (Shanghai, China). Tetramethylbenzidine (TMB) was bought from Macklin Biochemical Co., Ltd (Shanghai, China). Alcohol Dehydrogenase was purchased from Sigma-Aldrich (St. Louis, USA). The detection kits were obtained from Beyotime Biotechnology (Shanghai, China) including Reactive Oxygen Species Assay Kit, Mitochondrial Membrane Potential Assay Kit with Rhodamine 123, Hoechst Staining Kit, NAD^+/NADH Assay Kit with WST-8 and $NADP^+$/NADPH Assay Kit with WST-8. Anti-SIRT7antibody (AF7986, 1:1000) rabbit polyclonal antibody was purchased from Beyotime Biotechnology (Shanghai, China). Anti-AKT antibody (60203-2-AP, 1:1000), anti-GSK3β antibody (22104-1-AP, 1:1000), p- AKT antibody (80455-1-Ig, 1:1000), rabbit IgG, anti-actin antibody (81115-1-Ig, 1:5000) and mouse IgG were purchased from Protein-tech Group (Wuhan, China). p-GSK3β antibody (bs-5367R, 1:1000) were obtained from Bioss Biotech Co., Ltd. (Beijing, China). Coomassie Plus (Bradford) Assay Kit was purchased from Thermo scientific (Massachusetts, USA). Commercially available reagents were analytical grade and used without further purification. All aqueous solutions were prepared with deionized water (18.2 MΩ·cm, Millipore).

2. Instrumentations

Scanning electron microscopy (SEM) observation and Energy-dispersive X-ray spectroscopy (EDX) elemental mapping were performed on an XL-30 ESEM FEG instrument (FEI, Hillsboro, Oregon, USA). Transmission electron microscopy (TEM) images were measured using a JEM-2100 PLUS transmission electron microscope (JEOL Ltd., Japan) operating at 200 kV. X-ray photoelectron spectroscopy (XPS) was obtained using an ESCALAB-MKII spectrometer (VG Co., United Kingdom) with Al Kα X-ray radiation as the X-ray source for excitation. The crystalline structure was characterized by X-ray diffractometer (XRD, Bruker D8 ADVANCE, Germany). The nitrogen (N_2) adsorption desorption isotherms were measured by ASAP 2020 instrument (Micromeritics, USA). Raman spectra were obtained on Renishaw Raman system model 1000 spectrometer. Ultraviolet-visible (UV-Vis) absorption measurements were collected on a SparkTM Multimode Microplate reader (Tecan, Männedorf, Switzerland) and Nanodrop OneC (Thermo Fisher Scientific, Inc., Wilmington, DE, U.S.A.).

3. Synthesis of C@Co nanozyme

Typically, 10-20 g of NaCl salt, 0.41 g of sucrose, 5 g of imidazole, and 1.62 g of $Co(NO_3)_2 \cdot 6H_2O$ were frozen into a solid state using liquid nitrogen for several minutes. The ice cube was then freeze-dried multiple times to remove water. The resulting powder mixture was transferred to a tube furnace with a H_2 flow and subsequently underwent pyrolysis at 900 ^oC for 2 h at a heating rate of 5 ^oC/min. The nanozyme was

obtained after washing three times. The sample without adding cobalt was synthesized at 900 ^{o}C.

4. NAD(P)H oxidase mimicking activity of C@Co

In a representative experiment, NAD(P)H and C@Co were sequentially introduced into a vial containing 930 μL of 10 mM HEPES buffer (pH 7.4). The final concentrations of NAD(P)H and C@Co were set at 0.1 mM and 20 μg/mL, respectively. Following a 60-min incubation at room temperature, 20 μL of HRP (0.1 mg/mL) and 20 μL of TMB (20 mM) were added to the solution. UV-vis absorption measurements were taken within 30 s. For the NADH regeneration experiment, ADH (0.2 U) and ethanol were introduced to the mixture after the removal of C@Co.

5. Kinetics assays

Steady-state kinetics assays were performed at room temperature using 1.0 mL cuvettes with a path length of 1.0 cm. The reactions took place in a 10 mM HEPES buffer (pH 7.4). For the kinetics assays, a final concentration of 20 μg/mL for the nanozymes was maintained. Kinetic measurements were initiated after a 5-min illumination period. To obtain the kinetics data, the concentration of NAD(P)H was varied while maintaining a constant nanozyme concentration. Within the appropriate substrate concentration range, characteristic Michaelis-Menten curves were observed.

6. Intracellular NAD(P)H content

HeLa cells were seeded at a density of 10^6 cells/well in 6-well culture plates, each containing 2 mL of DMEM. After allowing 24 h for cell attachment, the DMEM was refreshed and supplemented with C@Co at a concentration of 100 μg/mL. Following a

12-h incubation with C@Co, the intracellular levels of NAD(P)H were measured using the NAD(P)H Assay Kit with WST-8.

7. MTT assay

Cell viability was assessed using the MTT assay. Initially, 2,000 cells were seeded per well in a 96-well tissue culture plate. Subsequent to this, various concentrations of the C@Co nano enzyme were introduced into each well, followed by incubation periods of 24 and 48 h. Upon completion of the incubation, the MTT assay was carried out using a detection kit provided by Beijing Solarbio Science & Technology Co., Ltd. (Beijing, China), strictly adhering to the manufacturer's guidelines. Absorbance was measured at OD570 nm to evaluate cell viability.

8. Colony formation assay

Cells were suspended in DMEM medium and seeded in a 6-well plate. After culturing at 37 ^{o}C for 24 h, they were treated either with PBS or the C@Co nano enzyme for an additional 24 h. Following this treatment, the cells were cultured for another 14 days, during which visible colonies formed. Once the medium was discarded, the cell colonies were fixed with 4% paraformaldehyde for 20 min. Subsequently, they were stained with 0.1% crystal violet for 20 min at room temperature and then imaged.

9. Confocal laser scanning microscopy

Two days prior to confocal laser scanning analysis, cells were pre-seeded on coverslips. Once they reached a confluence of 70-80%, they were treated with the C@Co nano enzyme for 48 h. Subsequent analyses for reactive oxygen species generation, mitochondrial membrane potential, and cell apoptosis were conducted

using the Reactive Oxygen Species Assay Kit, the Mitochondrial Membrane Potential Assay Kit with Rhodamine 123, and the Hoechst Staining Kit (all from Beyotime Biotech Co., Ltd., Shanghai, China), respectively, following the provided instructions. Images were captured using a laser scanning confocal microscope (Olympus, Shinjuku, Tokyo).

10. Quantitative real-time PCR (qPCR)

Total RNA was isolated from cells using the TRIzol reagent (Invitrogen, USA) and converted to cDNA as per the manufacturer's guidelines. Primers for qPCR were crafted utilizing Primer 5.0 software and synthesized by Sangon Biotech Co., Ltd. (Shanghai, China). mRNA expression was assessed in triplicates utilizing the SYBR Green I dye technique, with β-actin serving as the reference gene. The qPCR mix comprised 1 μL of cDNA, 5 μL of qPCR-Master Mix, 0.5 μL each of forward and reverse primers, and 3 μL of RNase-free H_2O, totaling 10 μL. The qPCR cycling conditions were: initial denaturation at 95 ℃ for 1 min, 40 cycles of 95 ℃ for 15 s, 60 ℃ for 15 s, and 72 ℃ for 15 s. Post-amplification, a melting curve analysis from 60 ℃ to 95 ℃ was conducted, and the amplified products were stored at 4 ℃. Data from the Eppendorf real-time PCR device (Hamburg, Germany) were processed using the $2^{-\triangle\triangle CT}$ method.

11. Western blot analysis

The protein concentration was quantified with the BCA protein assay kit (Boster, Wuhan, China). A total of 35 μg protein from each sample was separated using SDS-PAGE and subsequently transferred to PVDF membranes (Bio-Rad Laboratories Inc,

USA). For immunoblotting, primary antibodies were applied as per the manufacturer's recommended dilutions, using β-actin as the loading control. Detection of the immunoblots was performed using the ECL advanced western blotting detection kit (Invitrogen, USA).

12. Tumor xenograft

All animal experiments were approved by the Changchun Institute of Applied Chemistry, Chinese Academy of Sciences (Approval No. 20230001). Female BALB/c nude mice, aged 4-6 weeks, were acquired from the Charles River Animal Company of China and were randomly distributed into experimental groups, with six mice in each group. For the xenograft studies, an equal number of Hela cells were subcutaneously injected into the nude mice. Following three treatments on the xenograft tumors, tumor dimensions and weight were assessed using a caliper. Tumor volume was computed using the formula: volume = $1/2 \times ab^2$ (where "a" is the length and "b" is the width).

Ethics statement: all experiments were carried out in accordance with the guidelines laid down by the Institutional Animal Care and Use Committee of CIAC (CIAC/IACUC, AP20230080) regarding the care and use of animals for experimental procedures.

13. H&E staining

Tumor tissues were excised and fixed in 4% paraformaldehyde for a duration of 24 h. Specimens from different tissue lobes were positioned in processing cassettes, dehydrated in a series of alcohol concentrations, and subsequently embedded in paraffin wax. Prior to immunostaining, tissue sections, 5 μm in thickness, were dewaxed using

xylene, rehydrated through decreasing alcohol concentrations, and rinsed in PBS. The sections were then stained with hematoxylin and eosin (H&E). Post-staining, sections underwent dehydration through graded concentrations of ethanol, followed by xylene. The Hematoxylin and Eosin Staining Kit was utilized as per the manufacturer's instructions (Beyotime Biotech Co., Ltd., Shanghai, China).

14. Data analysis

The data are represented as the mean ± standard deviation (s.d.) from three independent experiments. Statistical analyses were conducted using a two-sided Student’s t-test, one-way ANOVA, or Kaplan-Meier survival analysis. The level of significance was set at the probabilities of *$p < 0.05$, **$p < 0.01$, ***$p < 0.001$ and ****$p < 0.0001$.

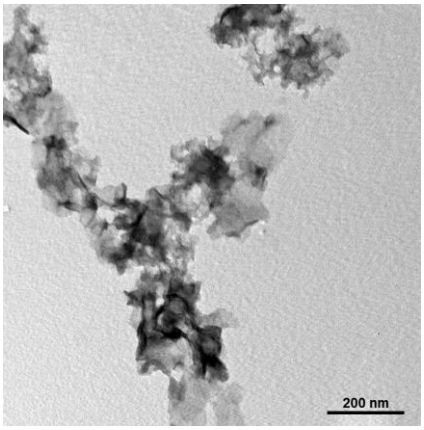

Fig S1. TEM image of the N-doped carbon matrix.

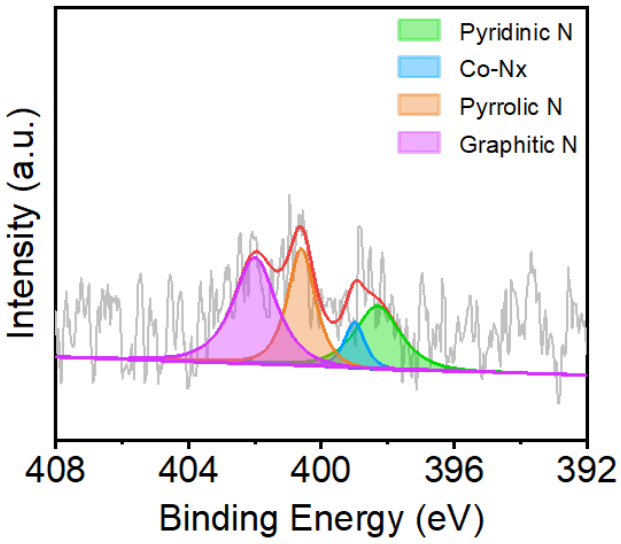

Figure S2. XPS spectra of the N 1*s* orbital.

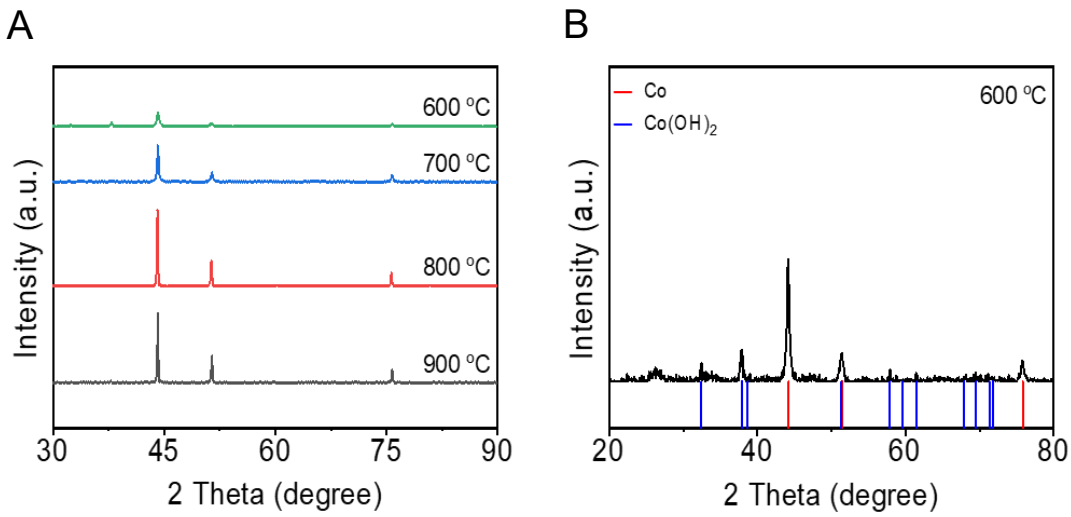

Figure S3. (A) XRD patterns of C@Co obtained at various carbonization temperatures and (B) pattern of C@Co at 600 ºC.

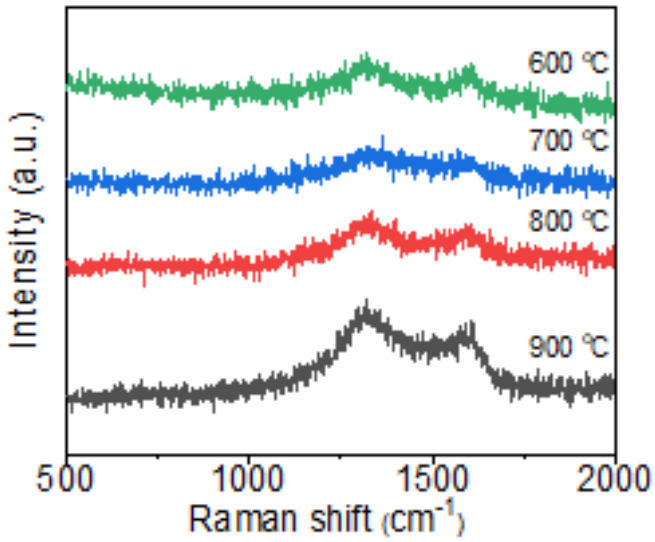

Figure S4. Raman spectrums of C@Co from different carbonization temperatures.

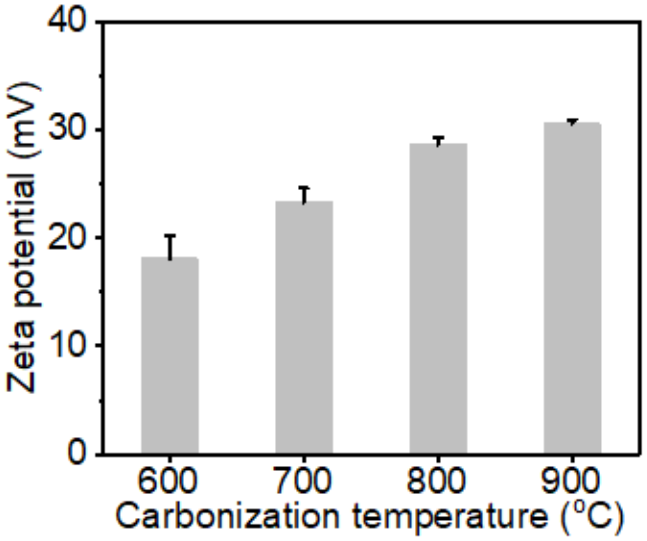

Figure S5. Zeta potential of C@Co measured at various carbonization temperatures.

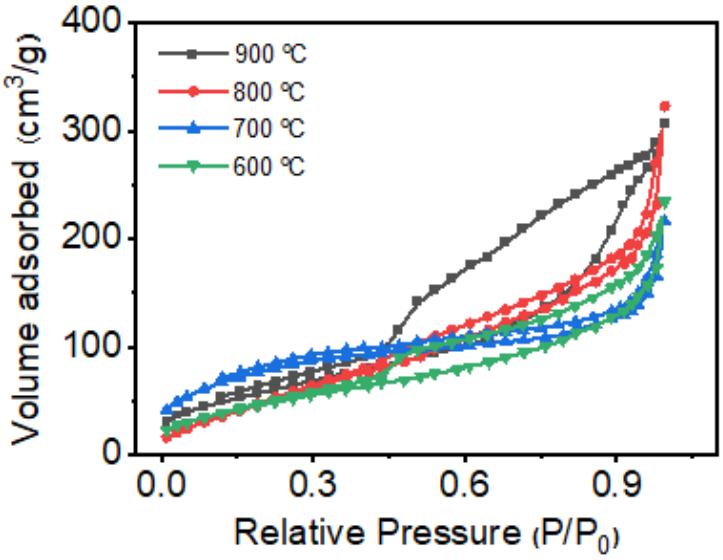

Figure S6. Nitrogen adsorption-desorption isotherms for C@Co obtained at different carbonization temperatures.

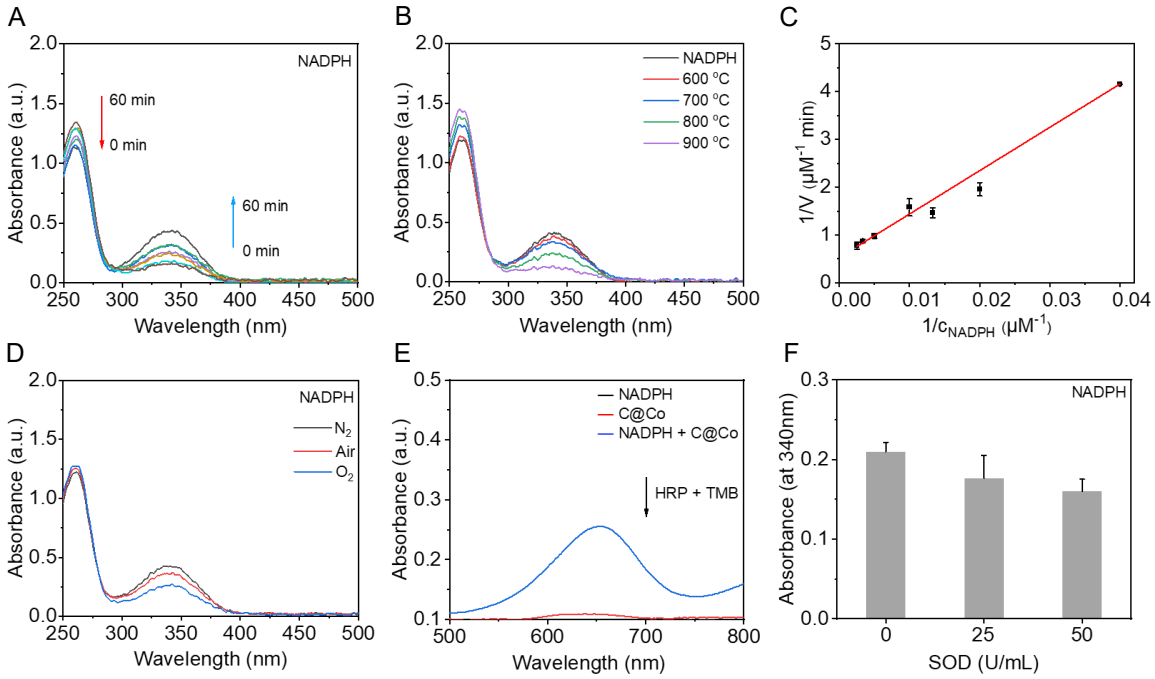

Figure S7. (A) UV-Vis spectra illustrating NADPH oxidation over time using the C@Co nanozyme. (B) UV-Vis spectra showing NADPH oxidation by C@Co from varying carbonization temperatures. (C) Double-reciprocal plots showcasing the activity of C@Co across different NADPH concentrations. (D) UV-Vis spectra of NADPH oxidation by C@Co in various gas environments. (E) UV-Vis spectra of assorted solutions post-addition of HRP and TMB. (F) The impact of the radical scavenger SOD on NADPH oxidation by C@Co.

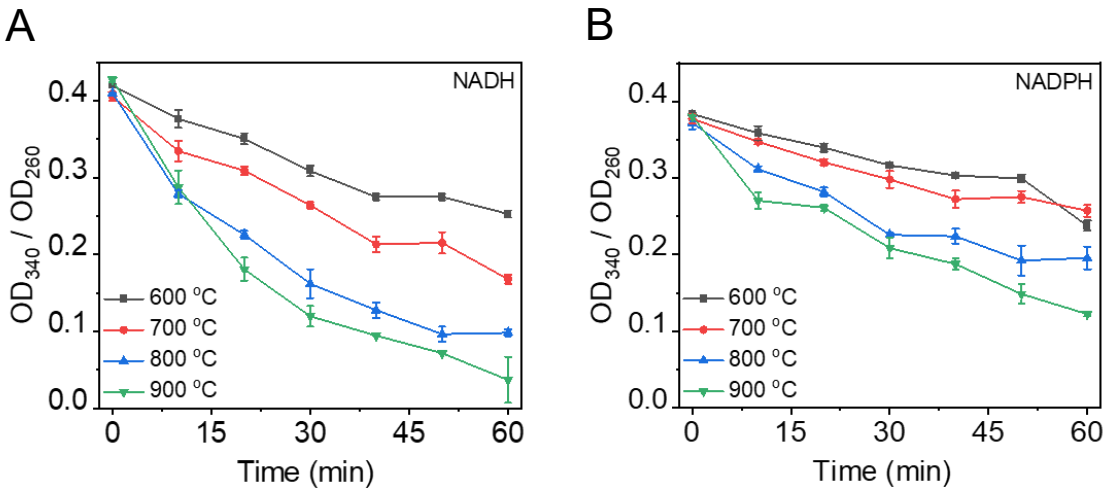

Figure S8. Time-dependent changes in the OD_{340}/OD_{260} ratio at 340 nm for (A) NADH and (B) NADPH.

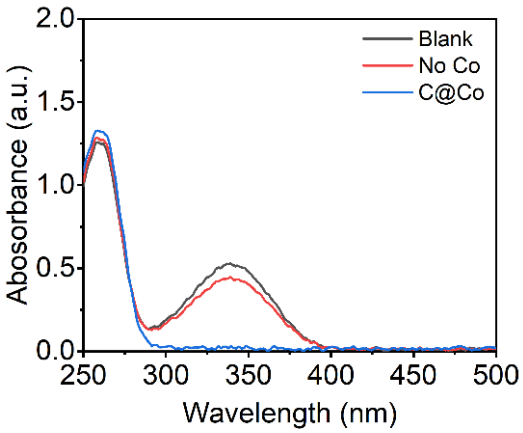

Figure S9. UV-Vis spectra representing NADH oxidation by the N-doped carbon matrix and C@Co.

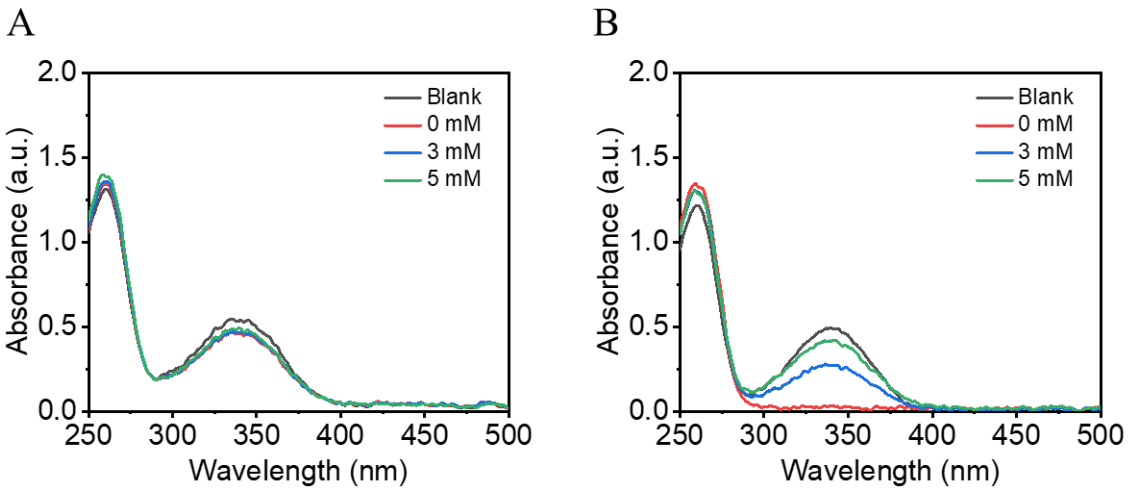

Figure S10. UV-Vis spectra changes of NADH upon the addition of various concentrations of KSCN by (A) the N-doped carbon matrix and (B) C@Co.

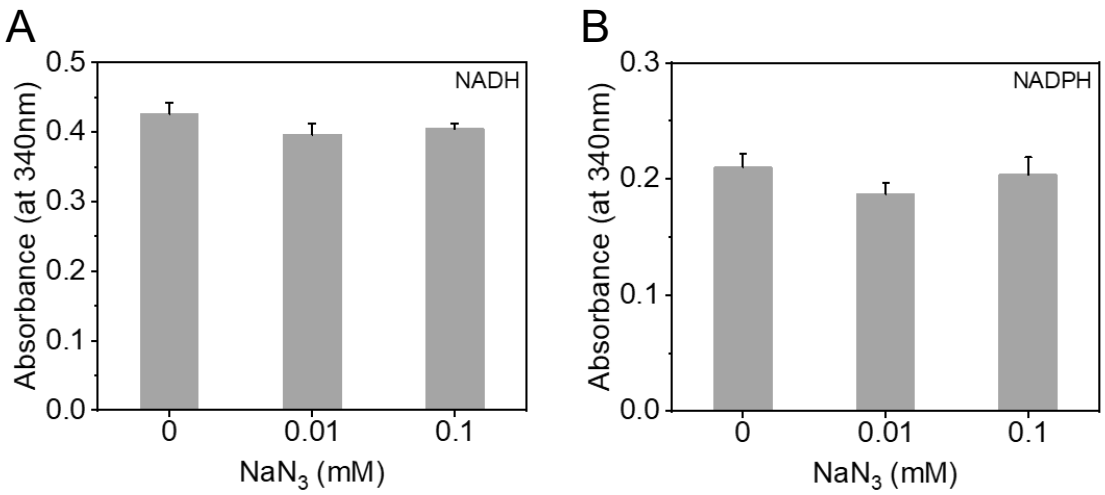

Figure S11. Influence of the radical scavenger SOD on the oxidation of (A) NADH and (B) NADPH by C@Co.

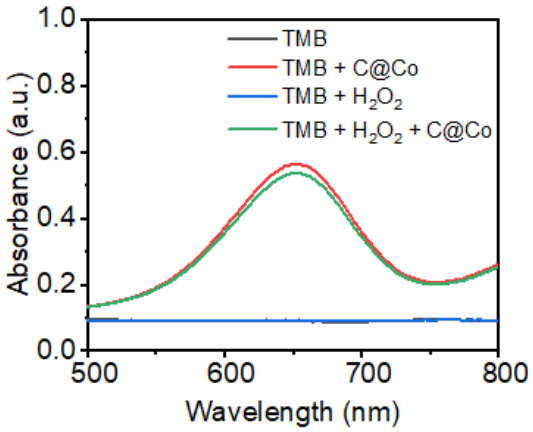

Figure S12. UV-Vis absorption spectra of various combinations: TMB alone, TMB with H_2O_2, TMB with C@Co, and TMB with both H_2O_2 and C@Co.

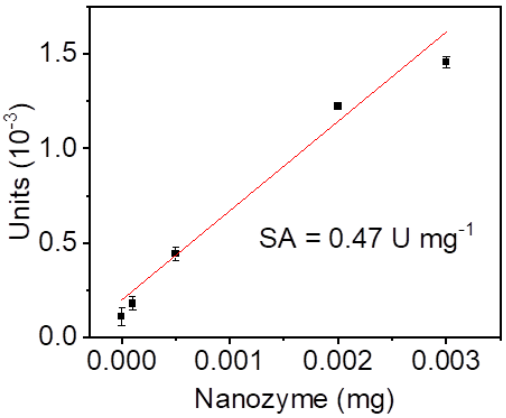

Figure S13. The specific activity value of C@Co.

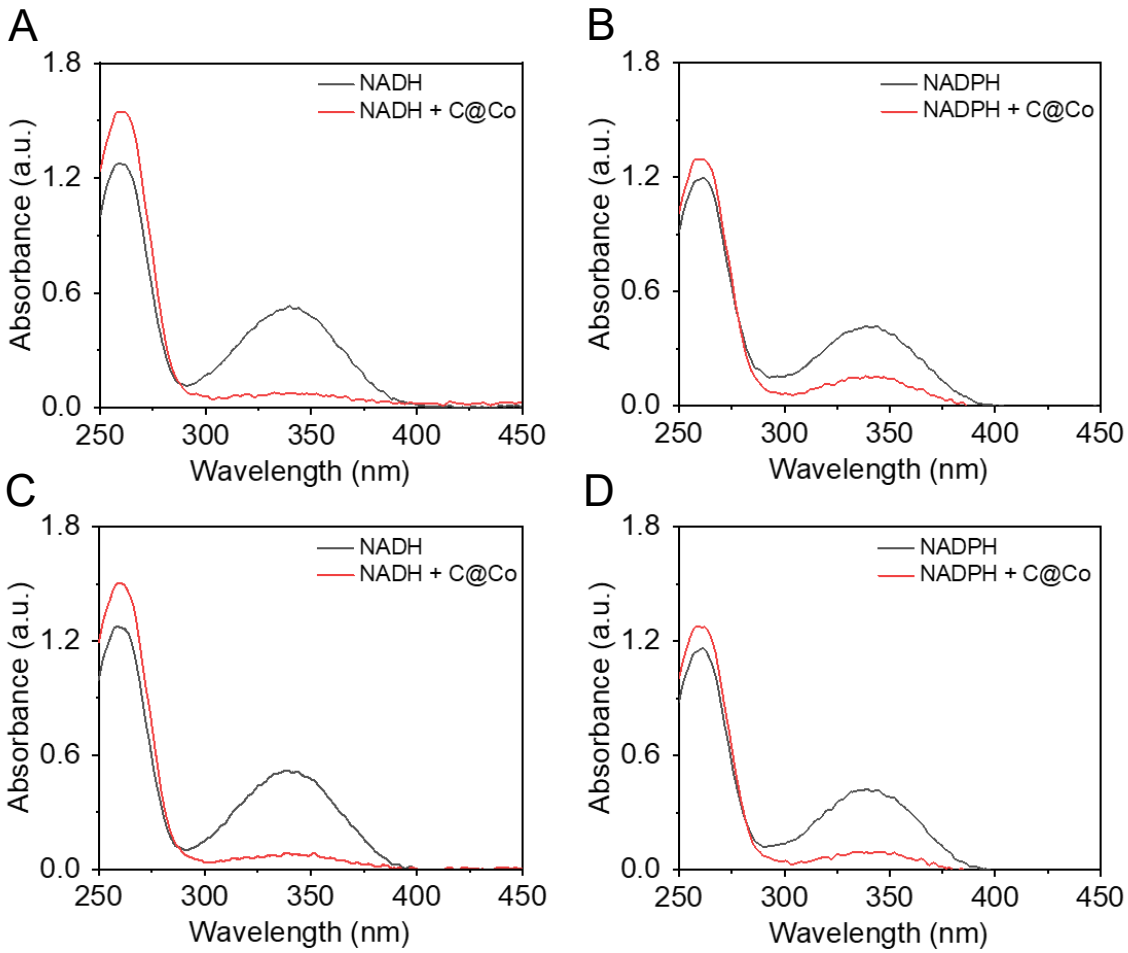

Figure S14. UV-Vis spectra of oxidation of NADH and NADPH by C@Co in different buffers. (A) NADH in HEPES buffer (10 mM, pH 7.4). (B) NADPH in HEPES buffer (10 mM, pH 7.4). (C) NADH in PBS buffer (10 mM, pH 7.4). (D) NADPH in PBS buffer (10 mM, pH 7.4).

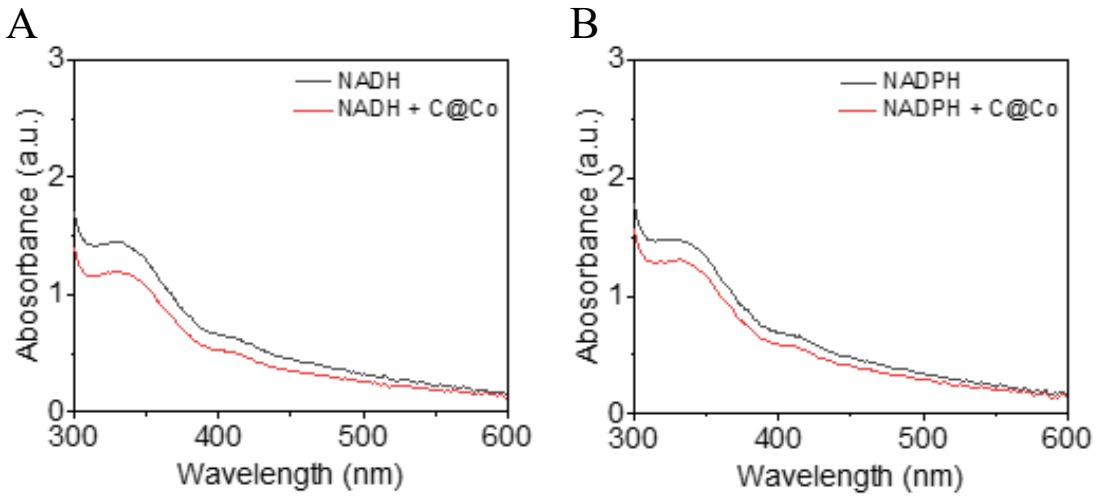

Figure S15. UV-Vis spectra illustrating the oxidation of NADH and NADPH by C@Co in a solution containing 10% FBS and 90% PBS.

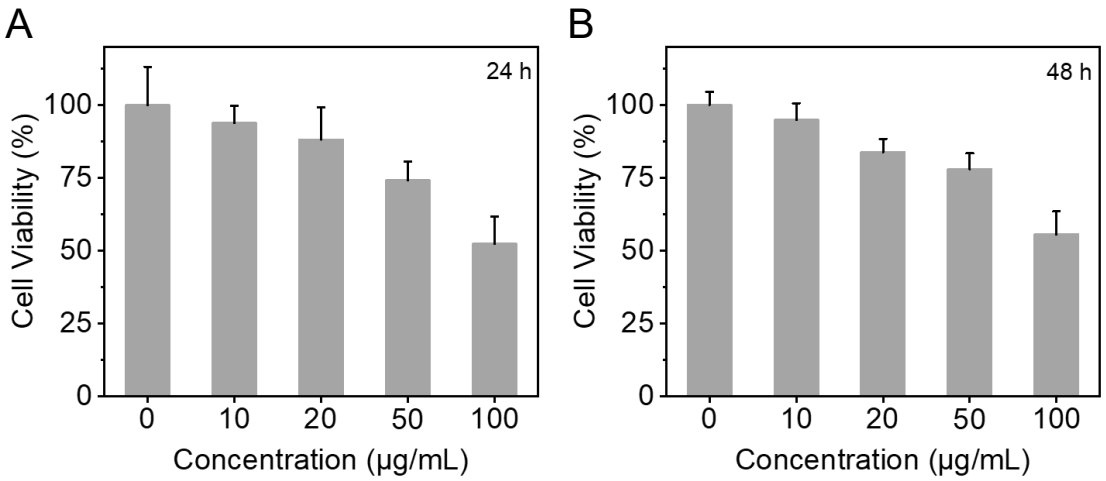

Figure S16. Cell viability of 293T cells exposed to varying concentrations of C@Co at 24 h (A) and 48 h (B).

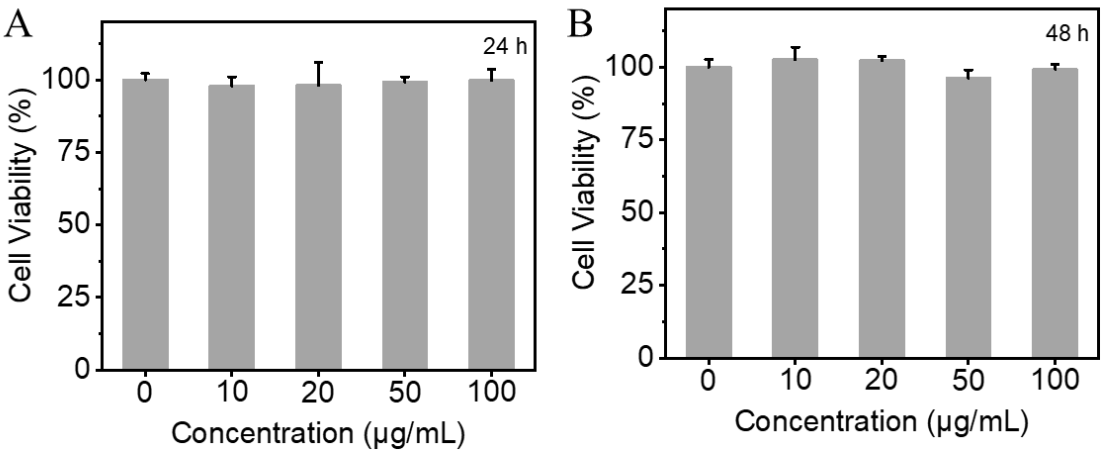

Figure S17. Cell viability of HeLa cells exposed to varying concentrations of the N-doped carbon matrix at 24 h (A) and 48 h (B).

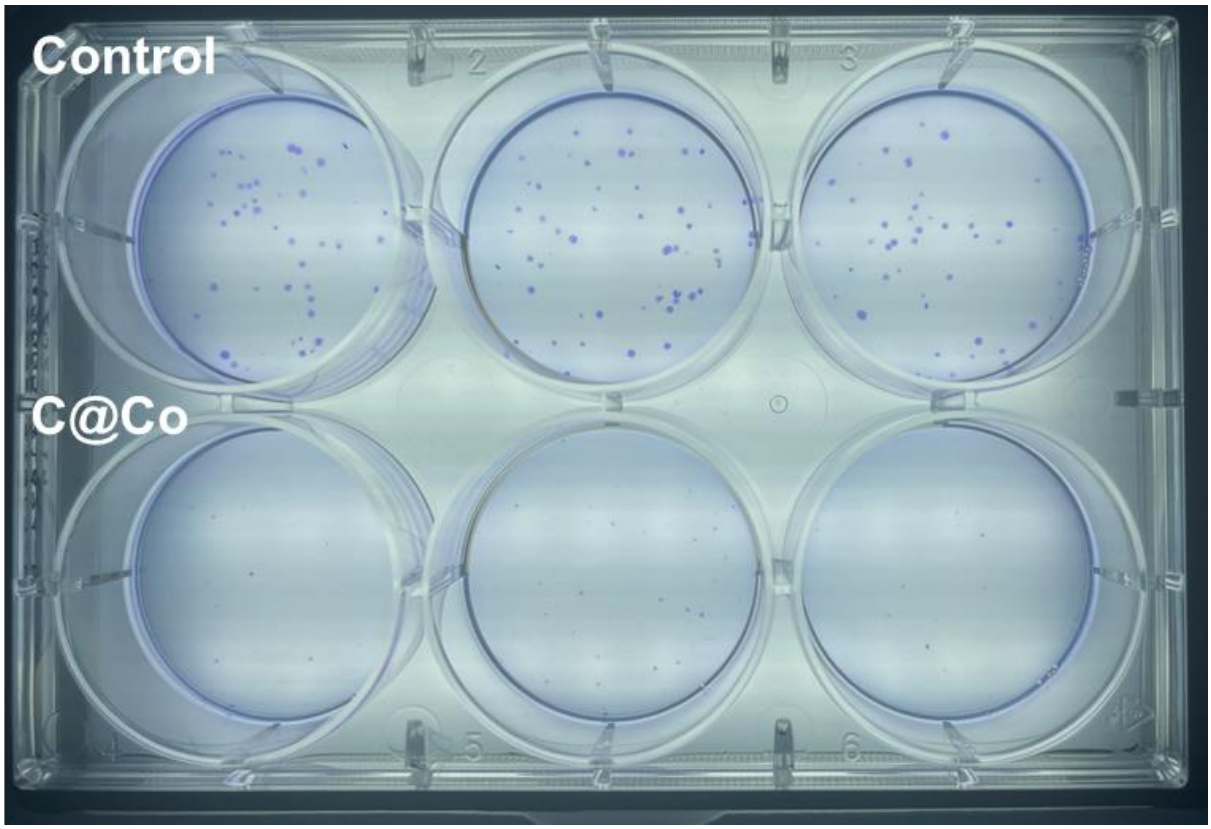

Figure S18. Colony formation assay of Hela cells following 14-day treatment with C@Co.

Table.S1 BET surface area, pore volume, and pore diameter values for C@Co derived at various carbonization temperatures.

Carbonization temperature	**BET area data (m^2/g)**	**Total pore volume (m^3/g)**	**Average pore diameter (nm)**
900 ℃	209.6	0.474	8.514
800 ℃	187.7	0.501	8.685
700 ℃	174.6	0.458	8.962
600 ℃	169.4	0.363	7.920